Symkom 2014 **Open Access**

Konrad Kacprzak* and Krzysztof Sobczak

Computational assessment of the influence of the overlap ratio on the power characteristics of a Classical Savonius wind turbine

DOI 10.1515/eng-2015-0039

Received December 08, 2014; accepted May 29, 2015

Abstract: An influence of the overlap on the performance of the Classical Savonius wind turbine was investigated. Unsteady two-dimensional numerical simulations were carried out for a wide range of overlap ratios. For selected configurations computation quality was verified by comparison with three-dimensional simulations and the wind tunnel experimental data available in literature. A satisfactory agreement was achieved. Power characteristics were determined for all the investigated overlap ratios for selected tip speed ratios. Obtained results indicate that the maximum device performance is achieved for the buckets overlap ratio close to 0.

Keywords: Savonius wind turbine; overlap; CFD

1 Introduction

The global small wind turbine (SWT) market has been growing steadily in the last years. The main reasons of this increase in the significance are the demand-supply gap in energy, increasing fossil fuel prices and improved small wind turbine technology as well as government regulations in different countries. To maximize the convertibility of wind energy, the major focus is on proper designs of wind turbine rotors and generators. Areas where wind speeds are relatively low and vary noticeably with seasons address specific demands. That is why conducting research on wind turbines, which can run in a low wind velocity and can be used in a small scale manner in remote and rural areas is crucial. A cheap and simple vertical axis wind turbine could be suitable for these conditions.

The Savonius wind turbine is a vertical axis wind turbine (VAWT) developed and patented by Sigurd J. Savonius in the 1920s. Due to the emerging market of so-called decentralised energy production, recently, there has been a steadily increasing interest in studies of the Savonius wind rotor. At the same time a lot of effort has been made to improve its aerodynamic performance.

This increased interest in the Savonius wind turbine derives directly from recognition of its main advantages like simple and cheap construction, high starting torque at low wind speeds, therefore it can be used in Darrieus-type wind rotor as a starter. It is also independent of the wind direction and the generator and gearbox can be placed on the ground or under the rotor, so the maintenance is cheap and convenient [1, 2]. All mentioned features together with a compact size of this kind of turbines make them suitable for the residential use. However, Savonius turbines exhibit small efficiency and low rotational speed [3, 4]. Therefore, constant search for better designs, in order to improve the performance of the rotor is vital.

A significant amount of performance data has been gathered [3, 5] by various researchers for a wide range of rotor geometries, but there is still no generally accepted value of overlap ratio to be used in designing an "optimum" rotor geometry. Part of the problem stems from the lack of standardisation of measurement and testing techniques utilised by different investigators. Another reason for this is an existence of unavoidable blockage effects which affect most data collected from tests in wind tunnels. Current development in Computational Fluid Dynamics (CFD) makes it possible to conduct a comprehensive study of different designs of the Savonius rotor without committing a significant amount of time and money for experimental investigations.

2 Studied geometry

In this paper the Classical rotor (Figure 1) was examined by means of numerical simulations. In order to investigate the influence of the overlap ratio on the power characteristics of a Classical Savonius wind turbine, full scale three-dimensional (3D) simulations were carried out together with a series of two-dimensional (2D) simulations. Dimensions of a numerical model directly correspond to a low

***Corresponding Author: Konrad Kacprzak:** Institute of Turbomachinery, Lodz University of Technology, Wólczańska 219/223, 90-924 Łódź, Poland, E-mail: kokacprzak@gmail.com

Krzysztof Sobczak: Institute of Turbomachinery, Lodz University of Technology, Wólczańska 219/223, 90-924 Łódź, Poland

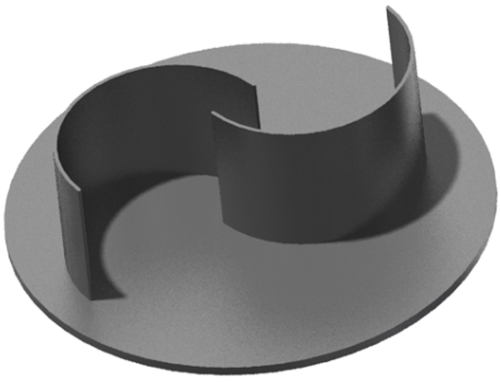

Figure 1: Model of the investigated Classical Savonius wind turbine (due to its symmetry only a half of turbine is presented).

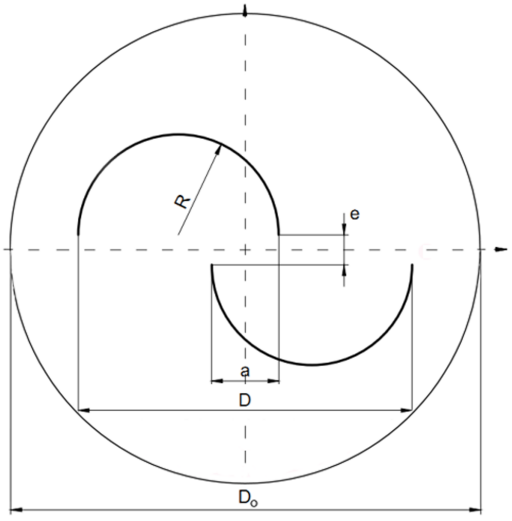

Figure 2: Geometrical parameters of the Classical Savonius wind turbine.

aspect ratio turbine examined experimentally by Kamoji *et al.* [5, 6]. In this way, it was possible to verify obtained results and check the influence of different task configurations (2D or 3D solutions) on the prediction quality. Simulations are conducted for a rotor with a height H = 0.154 m; diameter D = 0.2 m; aspect ratio H/D = 0.77; an end plate diameter Do/D = 1.33; the inter-blade distance e = 0 (Figure 2). The rotor overlap ratio was examined in the range: a/D = 0.0-0.3 (distance measured between the centre lines of the blades) for variable R and constant D. The blade thickness is equal to 2 mm.

3 Simulation definition

In this study both 2D and 3D simulations were carried out with ANSYS CFX. For the purposes of these investigations the model was composed of two domains (Figure 3). The first one (rotating) comprised the wind turbine blades and endplates and the second (stationary), simulated the wind tunnel with dimensions in accordance with the experimental test stand data [5, 6]. The rotating domain radius was twice as big as the rotor radius. Such a domain size was chosen in order to assure that vortex structures in a close vicinity of the rotor are solved in a rotating frame of reference and it also minimised numerical errors due to numerous transitions of fluid through the domain interface. Due to the rotor symmetry, only a half of the turbine was solved. Simulation definition in the case of 2D model was similar, however, due to a nature of the ANSYS CFX solver, a slice (1 mm thickness) of 3D domain near the symmetry plane was used.

Meshes for the given geometry were prepared using Meshing software in ANSYS Workbench. In the performed simulations a high-quality, unstructured, hexahedral mesh was utilised. Described grid was comprised of hexahedral layers, perpendicular to the rotor axis. Throughout the analysis different mesh densities were employed. In case of the 3D mesh $\sim 15 \cdot 10^6$ nodes) y+ values for the buckets were lower than 2, which made it possible to fully resolve the boundary layer, which due to considered flow structure is of a very high relevance. In the case of 2D simulation one element layer was applied with $\sim 5 \cdot 10^5$ nodes.

Taking into account low wind speed in the described case, density changes were relatively low, that is why, it was assumed that air in this case is incompressible. Due to constant changes of the blade position in reference to the wind direction, the flow structure is very complex and extensive separations occur. Hence, the unsteady Reynolds Averaged Navier-Stokes (RANS) simulations and especially turbulence modelling in this case is a challenge. In the described simulations Shear Stress Transport (SST) turbulence model was utilised. It was successfully used in similar studies [7, 8]. The selection of this two-equation model was based on the fact that it was designed to give accurate prediction of the flow separation regions under the adverse pressure gradients, when an adequate mesh refinement (as in this study) is applied. It is achieved by an implementation of the transport effects to the formulation of the eddy viscosity. That is why, it is used whenever a

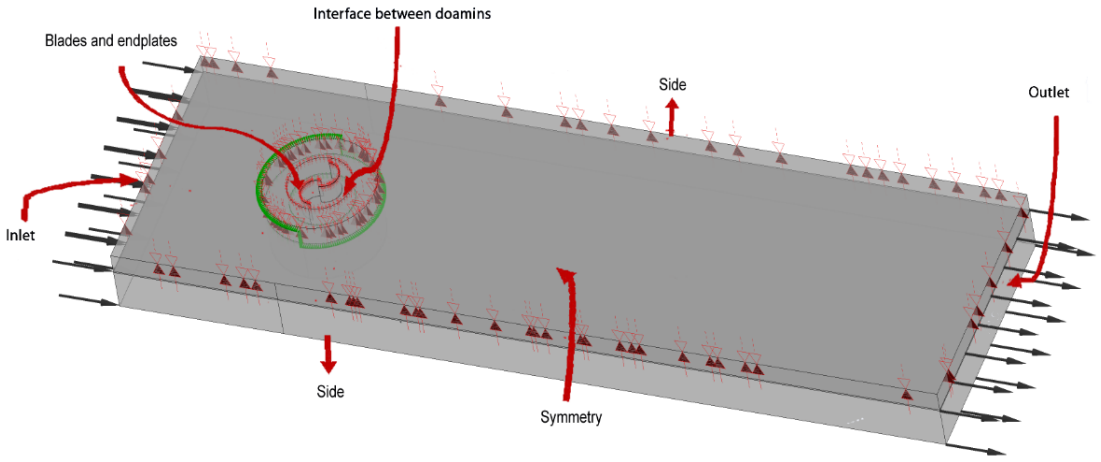

Figure 3: Orthogonal projection of 3D simulation domain.

high boundary layer accuracy is required[1], which is a case in this investigation. Utilising this turbulence model also enabled the laminar-turbulent (LT) transition modelling. The $\gamma - \theta$ model was applied[1], which was demonstrated by numerical studies [9] to have a positive influence on the results agreement with the experimental data. This approach required such a mesh refinement to fulfil condition y+ < 1 (2). This condition was reached for the buckets both for 3D and 2D simulations. In the case of endplates, due to the fact that the LT transition is not of such a high importance in this region and taking into account the calculation time, y+ values were higher and wall function was applied[1].

At the inlet to the computational domain a wind velocity (9 m/s) boundary condition was imposed. This velocity corresponds to Re = 120 000. Additionally, low turbulence intensity (1%) was set as in [6]. At the outlet atmospheric pressure was imposed (10^5 Pa). Due to the fact that the turbine as well as the expected flow structure have a symmetry plane in the middle of the turbine height, in 3D simulations a symmetry boundary condition was set on this plane. In the case of 2D calculations, symmetry was imposed on both sides of the modelled layer, which is the typical approach in 2D simulations in ANSYS CFX. For turbine blades and endplates no-slip wall boundary condition was assumed (zero velocity on the wall surface). At sides and bottom of the domain (away from the rotor) the free-slip wall condition was imposed which direct the flow parallel to them without friction effects.

Adjusting the rotational velocity of the rotor made it possible to investigate different tip speed ratios:

$$TSR = \frac{\omega \cdot R}{U}, \tag{1}$$

where ω – turbine angular velocity, R – turbine radius, U – wind speed. In order to achieve conformity between mesh cells (360 uniform divisions) on two sides of the interface between the stationary and rotational domains, timestep for every tip speed ratio TSR was adjusted to achieve precisely 360 timesteps per one revolution.

ANSYS CFX uses an element-based finite volume method[1]. Second order advection (high resolution) scheme were utilised. Second order Backward Euler method was used for discretization of time terms. In order to properly control convergence, the level of the residual target was set to 10^{-5}, with a number of iterations for each timestep (so called internal convergence loops) between 310. In practice 6 iterations was necessary to reach the specified residual level. For selected time steps the root mean square Courant number equal to 3 were not exceeded. That implies that the timestep is small enough to adequately resolve important unsteady structures. It has to be mentioned that the results after 6-8 revolutions of the rotor yielded repeatable cycles. Thus, the data beyond the eighth revolution was taken into account during the post-processing of the solution results.

4 Simulation results

In order to verify the results of conducted simulations, obtained data were confronted with the experiment re-

1 ANSYS CFX v15 Help

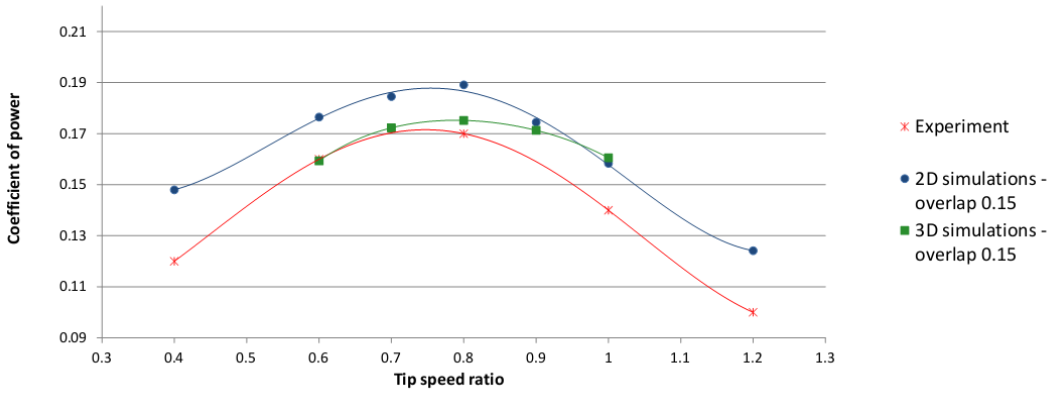

Figure 4: Comparison of the C_p coefficient from simulations and experiment

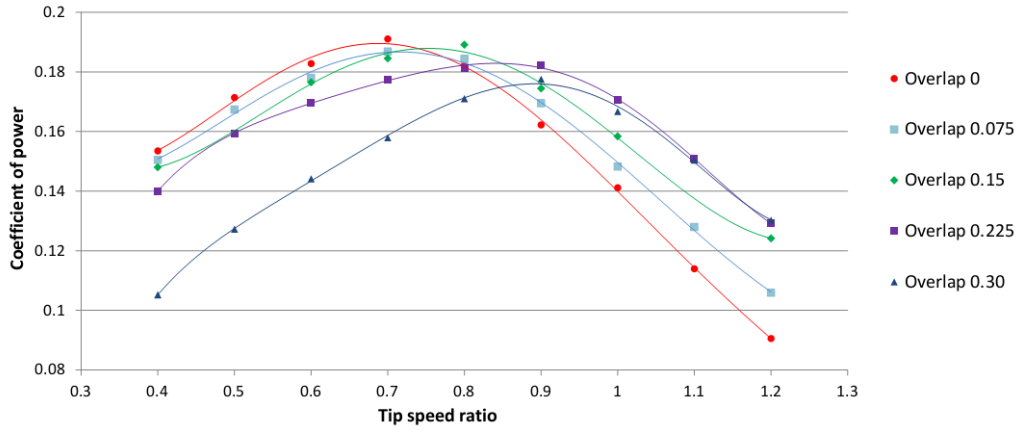

Figure 5: Coefficient of power for the Classical Savonius with different overlap ratios in 2D.

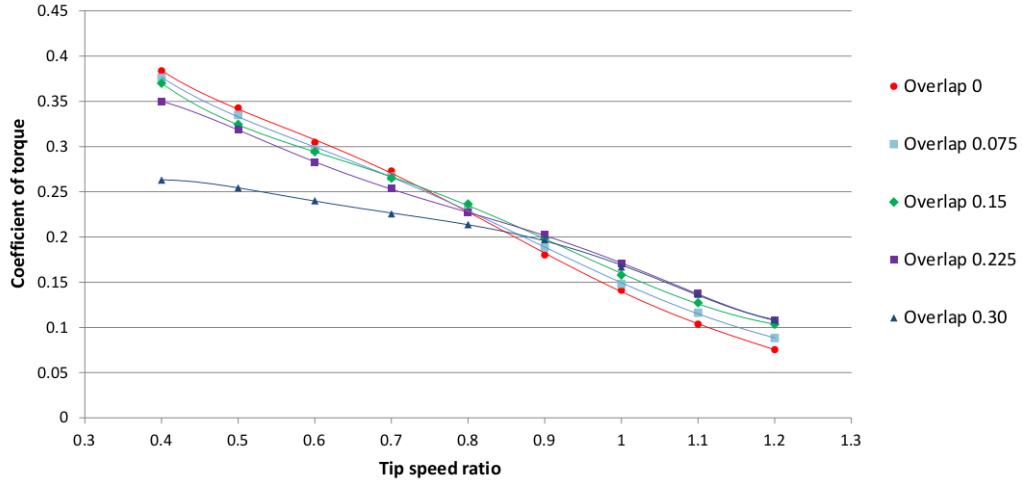

Figure 6: Coefficient of torque for the Classical Savonius with different overlap ratios in 2D.

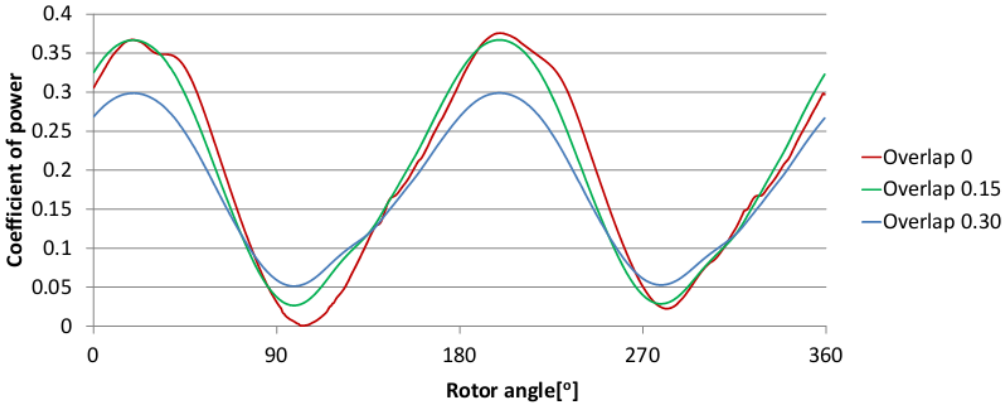

Figure 7: Coefficient of power for the Classical Savonius wind turbines with different overlap ratios versus angular rotor position at TSR = 0.8.

sults from Kamoji *et al.* [5]. Relation between coefficient of power C_P (ratio of the rotor and wind power) and tip speed ratio TSR for the Classical Savonius wind turbine with the overlap ratio equal to 0.15 (which was reported to exhibit the highest C_P [5]), investigated by Kamoji *et al.* is presented in Figure 4, together with 2D and 3D simulation results.

$$C_p = \frac{2T \cdot \omega}{\rho \cdot U^3 \cdot D \cdot H}, \tag{2}$$

where: T – torque, ρ – air density.

It can be seen that 3D simulation results are in a good agreement with the experimental data for lower TSR, however with its increase, discrepancy from the experimental values seems to also increase. In case of 2D simulations overprediction of the results is higher. It could be expected that one of the aspects which result in overprediction of power of 2D solution is variation of air flow through the slot along the height of the turbine. However, 3D simulations revealed that apart from the vicinity of the endplates, the flow is more or less uniform along the rotor height for its different angular positions. However, it can be noticed that this overprediction is relatively constant. That is why all further analysis was conducted for 2D simulations, enabling more computations to be done, due to the much lower task size of 2D cases in comparison to 3D ones. One of the most important reasons of higher C_p for 2D simulations is the fact that the end plate effects were not taken into account.

In order to compare the performance of the turbines under study the power and torque coefficients are presented for different overlap ratios (Figures 5 and 6). Figure 5 shows that all turbines achieve their peak performance for the tip speed ratio in range from 0.7 to 0.9. A very interesting fact is that the peak performance of a turbine moves towards higher TSR with an increase in the overlap ratio. The highest value of the power coefficient for the overlap ratio equal to 0 is obtained for TSR = 0.7, while for the overlap ratio equal to 0.30 the best performance is attained at TSR = 0.9. The highest value of the power coefficient is obtained for the rotor without the overlap. However, in the range of the overlap ratios from 0 to 0.15 differences of the maximal C_p are very small. As it was presented in Figure 4, 3D phenomena have their significant influence on the rotor performance. It can be expected that an impact of the overlap flow in the endplate region would be different for each overlap ratio. Therefore, only 3D analysis (experimental or numerical) can reveal the best configuration. For overlap ratios above 0.15 a decrease in the maximal value of the power coefficient is significant.

Almost linear relation of the torque coefficient C_t (ratio between available and effective torque) as a function of TSR is shown in Figure 6. In case of the overlap ratio of 0.30 a significant decrease of the torque is observed for lower TSRs and the values for the highest TSR stayed at the same level as for the overlap of 0.225. As one can see in the case of the overlaps from 0 to 0.15 torque coefficient characteristics intersects for TSR in the range of 0.7 – 0.8.

$$C_T = \frac{4T}{\rho \cdot U^2 \cdot D^2 \cdot H}. \tag{3}$$

Figure 7 presents the relation between the coefficient of power and the angular position of the Classical Savonius rotor for different overlap values. Data for single, representative revolution are shown. As one can see, the power output of the turbine is not constant but it changes for different positions of the rotor blades with respect to the wind direction. The highest power output is reached twice for one revolution (two blade rotor) for the angle close to 20° and 200° when the blades are almost aligned with the flow direction, whereas minima are reached for angular posi-

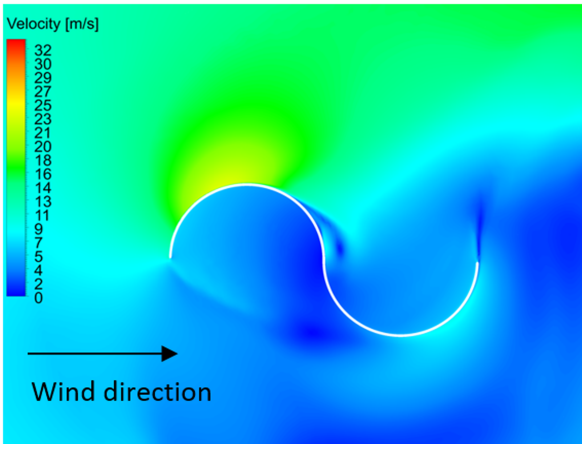

(a) no overlap

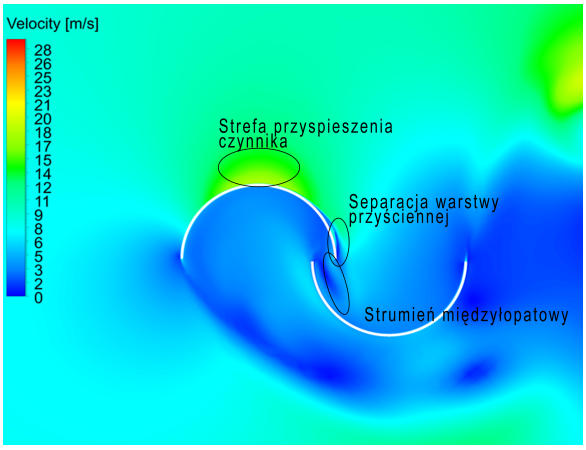

(b) overlap ratio = 0.075

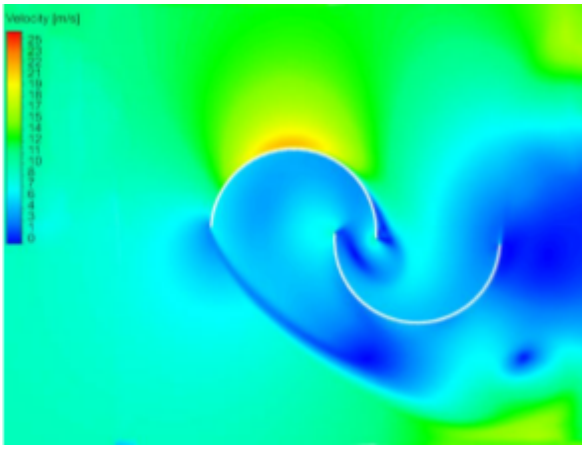

(c) overlap ratio = 0.15

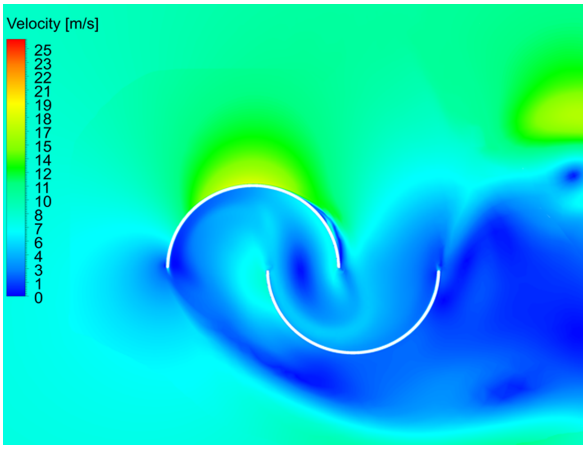

(d) overlap ratio = 0.225

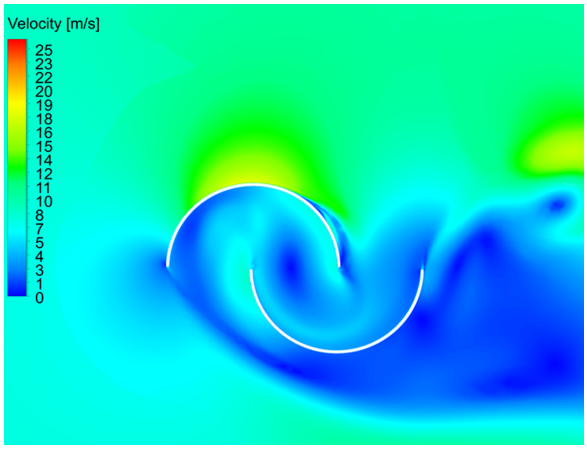

(e) overlap ratio = 0.30

Figure 8: Velocity distribution in stn. frame for different Savonius wind turbines at 0°.

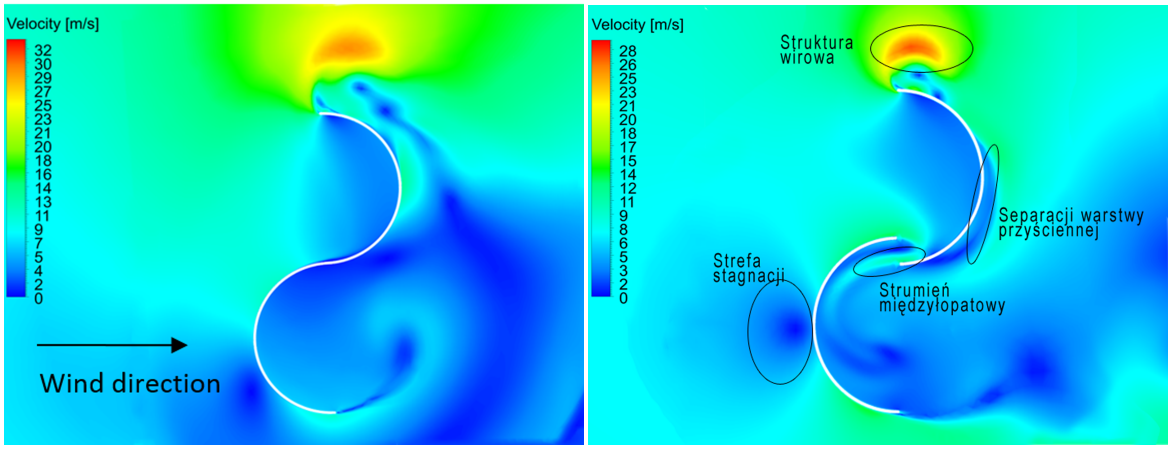

(a) no overlap (b) overlap ratio = 0.075

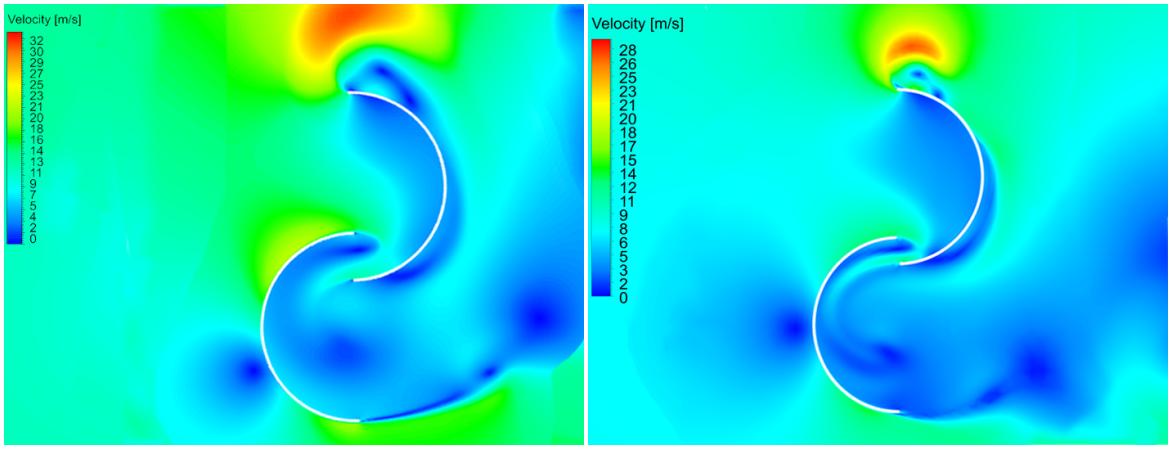

(c) overlap ratio = 0.15 (d) overlap ratio = 0.225

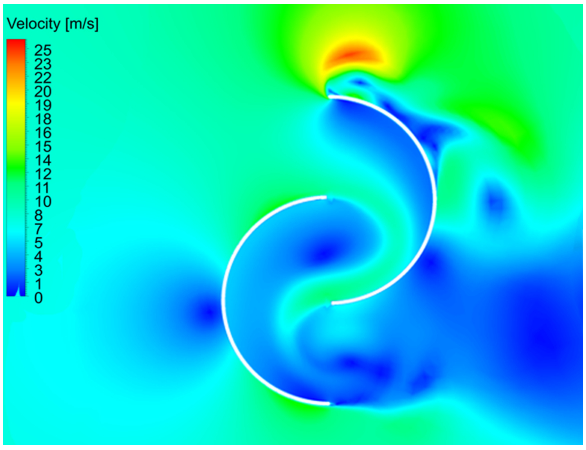

(e) overlap ratio = 0.30

Figure 9: Velocity distribution in stn. frame for different Savonius wind turbines 90°.

tions shifted by 90°. As far as the turbines with overlap ratios 0.15 and 0.30 are concerned two parts of the period are almost identical. In the case of the turbine without overlap some differences are observed, which can result from Magnus effect [10].

It can be noticed that the maximum values for overlaps 0 and 0.15 are similar, however, the first one attains its minimum close to $C_p = 0$. On the other hand, turbine with the highest overlap ratio (0.30) has the most stable power characteristics – the oscillation amplitude is the lowest, but as it was presented in Figure 5, the average power output and the magnitude of a torque coefficient are the smallest. It is also visible that in case of the turbine without an overlap the power characteristic has less uniform magnitude in every phase of the revolution. This may cause the material fatigue of the structural elements. Moreover, this kind of unstable behaviour can increase the noise production, which of course should be avoided.

In Figures 8 and 9 one can see that the flow structure is very complex and time dependent (fluid flows from the left-hand side). In the angular position 0° (Figure 8), when the relatively high torque is attained, a clear fluid acceleration on the convex side of the advancing blade (moving in agreement with the wind direction) is observed with subsequent separation of the boundary layer. This acceleration results in production of the lift force, which drives the turbine. This basic phenomenon coexists with numerous recirculation zones at the convex side of the advancing blade and both sides of the returning blade. According to Figure 9 in the angular position equal to 90° all rotors produce only a small amount of useful torque. Also, in case of rotors with an overlap ratio different than 0, a negative impact of the stagnation zone on the convex side of the returning blade is diminished to a certain extent by the overlap jet. The biggest differences can be seen in the magnitude of the velocity on the convex side of the advancing blade, and near the centre of the blades. The main reason of this fact is the influence of the gap of the Savonius rotor. As many researchers have reported [11, 12], the Coanda flow in the gap increases the torque. It can be seen that the main positive effect is a slight reduction of the negative torque produced close to the centre of the rotor.

Figure 9 presents turbines with different overlap ratios for the angular position for which the power output is almost the lowest. With the increase of the passage gap it can be noticed that for this rotor position also the overlap jet increases (positive influence on the performance of the rotor). However, together with the overlap jet also a vortex between blades increases. In this way, the effect of a positive moment induced by the overlap jet is diminished by a dissipative character of the vortex. It may be concluded that the best solution, from the efficiency point of view, would be to find a good balance between the magnitude of the overlap jet and a nearby vortex. It can be noticed in Figure [8] that for this rotor configuration it is rather difficult to spot a well-developed overlap jet. Nevertheless, vortices created with a contribution of the passage gap still remain in position. It suggests that in this configuration there is no beneficial effect of the passage gap itself, however, the lift force produced by the flow acceleration on the convex side of the advancing blade is a main driving factor for the turbine. The flow structure obtained in this numerical study directly corresponds to other research, in which the flow in the Bach-type Savonius wind turbine was studied by means of PIV [13].

5 Conclusions

On the basis of the performed numerical investigations the following conclusions can be drawn:

- Two-dimensional (2D) simulations of the Classical Savonius turbine overpredict the experimental data by constant value of the power coefficient in all the range of tip speed ratios (TSRs).
- Three-dimensional (3D) simulations perform much better for TSR below and close to nominal operation point but overprediction for higher TSRs is significant.
- The tip speed ratio (TSR) of the maximal power coefficient value increases with growth of the overlap ratio.
- In the range of the overlap ratios up to 0.15 the maximal value of the power coefficient stayed at constant level. A significant decrease is observed for the highest investigated overlap ratio (0.30).
- The overlap strongly influences the operation of the Savonius wind turbine. The intensity of the overlap flow increases with the overlap ratio.
- The overlap flow is the most significant for the rotor angular position when the torque/power is the lowest. In this case a strong jest is observed. However, it induces strong vortex structure which occupies significant part of the gap. For the angular position when the torque is the highest the jest is not observed and the gap vortex is of much lower intensity.

Acknowledgement: This article was funded from the public budget by the Ministry of Science and Higher Education as the "Diamond Grant" research project no. DI2011 000441.

References

[1] Spera D., Wind Turbine Technology: Fundamental Concepts of Wind Turbine Engineering. ASME Press, New York, 2009.
[2] Wagner H.J., Mathur J., Introduction to Wind Energy Systems: Basics, Technology and Operation. Green Energy and Technology, Springer, Heidelberg, 2009.
[3] Fujisawa N., Gotoh F., Experimental Study on the Aerodynamic Performance of a Savonius Rotor, J. Sol. Energy Eng., 1994, 116, 148–152.
[4] Ogawa T., Theoretical Study on the Flow about Savonius Rotor. J. Fluid. Eng. T. ASME, 1984, 106, 85–90.
[5] Kamoji L., Kedare S., Prabhu S., Experimental investigations on single stage modified Savonius rotor. Appl. Energy, 2009, 86, 1064–1073.
[6] Kamoji L., Kedare S., Prabhu S., Experimental investigation on single stage, two stage and three stage conventional Savonius rotor. Int. J. Energ. Res., 2008, 877–895.
[7] Zhao Z., Zheng Y., Xu X., Research on the improvement of the performance of Savonius rotor based on numerical study, Sustainable Power Generation and Supply, 2009. SUPERGEN'09. International Conference, Nanjing, April 6-7, 2009.
[8] Zhou T. and Rempfer D., Numerical study of detailed flow field and performance of Savonius wind turbines. Renew. Ener. 2013, 51, 373–381.
[9] Kacprzak K., Liśkiewicz G., Sobczak K., Numerical investigation of conventional and modified Savonius wind turbines. Renew. Energ., 2013, 60, 578–585.
[10] Shigetomi A., Murai Y., Tasaka Y., Takeda Y. Interactive flow field around two Savonius turbines. Renew. Energ., 2011, 36, 536–545.
[11] Fujisawa N., Velocity measurements and numerical calculations of flow fields around Savonius rotors. Exp. Fluids, 1996, 59, 711–720.
[12] Zhou T., Rempfer D., Numerical study of detailed flow field and performance of Savonius wind turbines. Renew. Energ., 2013, 51, 373–381.
[13] Dobreva I., Massouha F., CFD and PIV investigation of unsteady flow through Savonius wind turbine. J. Wind Eng. Ind. Aerod., 1996, 6, 39–50.